Akram O. Kadhum[1], Abbas S. AL-Ameeri[1], Shaker J. Edrees[2]*

[1]Department of Civil Engineering, College of Engineering, University of Babylon, Iraq, [2]Department of Ceramic and Building Materials, College of Materials Engineering, University of Babylon, Iraq

Scientificpaper
ISSN 0351-9465, E-ISSN 2466-2585
https://doi.org/10.62638/ZasMat1325

Zastita Materijala 66 (4)
845 - 866 (2025)

High-performance eco-friendly concrete with improved strength, chloride ion penetration, and corrosion resistance by the high volume of Ground Granulate Blast Furnace Slag (GGBS)

ABSTRACT

The present research aims to manufacture concrete that meets compressive strength parameters, has the lowest environmental impact, and resists chloride ion penetration and corrosion. This study used varied volumes of cement replacement with slag (GGBS) (30, 40, and 50)% by mass of cement for two concrete classes, C30 and C40. Fresh tests (slump, initial and final setting time), hardening (compressive, splitting, and flexural strength), and durability (porosity, water absorption, density, penetration depth, chloride ion migration coefficient, electrical resistivity, corrosion rate, mass loss, crack width due to corrosion, and microstructure analysis) were performed.

The environmental impact of concrete components in each mix was also assessed. The impressed current technique increased rebar corrosion in concrete specimens immersed in 5% sodium chloride. Replacing cement with GGBS by 30–50% increased the setting time and enhanced all hardening qualities. Mechanical qualities improved most at 40% GGBS, with C30 mixes' compressive, tensile, and flexural strengths up 29.3%, 38.7%, and 15.8% at 90 days. Compare 21.3%, 19.2%, and 16.2% at 90 days for C40 combinations to the reference mixture. Strength reduced marginally at 50% GGBS but remained greater than the reference blend. However, a 50% GGBS replacement rate best-improved durability, microstructure, and environmental efficiency. The C30-50% GGBS mixture is ideal because it met the design requirements of C30 and C40, had the best improvement in porosity and water absorption, the slightest chloride penetration, and the best performance against corrosive environments of the six mixtures except C40-50% GGBS. Additionally, it is the least environmentally harmful combination.

***Keywords**: GGBS; Chloride ion penetration; Corrosion resistance; microstructure of concrete; environmental impact; Durability*

1. INTRODUCTION

Concrete is an essential component of global civil construction systems and the most extensively used building material, particularly valued for its robustness, affordability, resistance to water infiltration, and flexibility[1]. It accounts for 66% of the total construction materials used worldwide, resulting in excessive cement manufacturing[2], Consequently, this phenomenon exacerbates environmental issues such as water contamination, carbon dioxide release, and depletion of resources [3].In order to promote worldwide sustainability, mitigate the manufacturing of raw materials, and minimize their environmental consequences, it is imperative to enhance concrete durability [4,5]. Chloride-induced steel corrosion is a crucial determinant of concrete durability [6,7,8]. Numerous developed countries experience significant economic losses as a result of infrastructure deterioration caused by corrosion. More precisely, the United States experiences an approximate yearly expenditure of $240 billion due to damage caused by corrosion, with around 20% of this cost being ascribed to the corrosion of reinforced concrete [9,10]. Furthermore, the economic consequences of corrosion on structures in South Korea, Middle Eastern countries, and other developed nations are estimated to be (2.9, 5.2, and 3.8)% of their respective domestic financial resources, respectively [11]. Consequently, infrastructure management authorities in many nations are actively increasing their efforts to

*Corresponding author: Akram O. Kadhum
E-mail:akram.kadhum.engh363@student.uobabylon.edu.iq
Paper received: 21. 12. 2024.
Paper accepted:15. 01. 2025.

evaluate the state of concrete structures. This requires monitoring for structural integrity and longevity and, if needed, establishing suitable maintenance procedures [12,13]. The implementation of proactive management strategies serves to prolong the lifespan of infrastructure and mitigate the environmental and social consequences..

As depicted in Figure 1, the degradation of concrete caused by chloride follows a sequential process consisting of three phases: initiation, rust propagation, and corrosion acceleration[14]. Corrosion of rebar in concrete initiates when the protective oxide layer (Fe_2O_3) loses its stability and is penetrated by chloride ions upon migration[15]. Upon this disturbance, the process of rust spreading begins, and the resulting corrosion products become apparent on the surface of the rebar. It is possible for the iron in steel to undergo oxidation up to six times its initial volume[16], which greatly increases the tensile stress in the concrete and results in the formation of microcracks and internal cavities[17]. The proliferation of microcracks promotes the continued entry of chloride ions, which, in turn enhances the penetrability of concrete and the infiltration of moisture that may transport other harmful chemicals. Consequently, this accelerates the corrosion of reinforce bars. In the absence of prompt maintenance, structural failure may occur due to the manifestation of severe deterioration, including surface-breaking cracks, spalling, and delamination [17,18]. In addition, Figure 1 illustrates a significant rise in maintenance expenses throughout the period of accelerated concrete degradation[14]. Therefore, producing concrete with high resistance to the penetration of chloride ions has become imperative, and it can be possible only by reducing the permeability of the concrete [20].

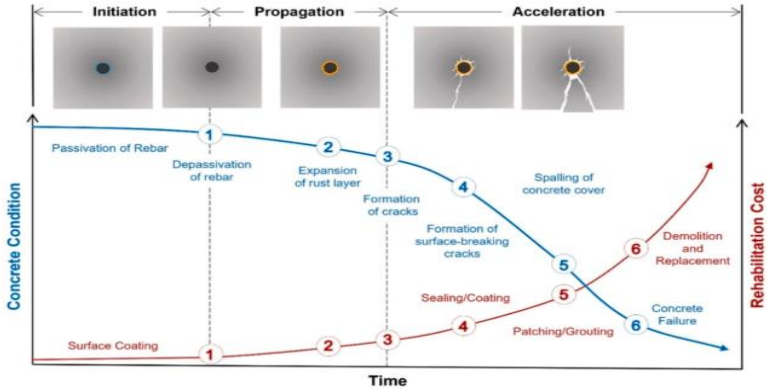

Figure 1. Conceptual model of steel corrosion-induced concrete deterioration and rehabilitation costs [18]

Utilizing different supplementary cementitious materials (SCM) to produce blended cement contributes to achieving durable and sustainable concrete[21]. Partial cement replacement with SCM, such as GGBS, One of the most viable approaches for manufacturing more ecologically friendly and sustainable concrete with enhanced durability[22]. GGBS is a residual material generated during the manufacturing of pig iron. Every tonne of GGBS produced releases around 0.14 tonnes of CO_2. Comprising a mere 16%emissions of carbon dioxide resulting from cement manufacturing [23]. Therefore, the intensive utilization of high volume GGBS as a substitute for cement is a successful approach to manufacture eco-friendly construction materials and fulfill the criteria of sustainable development[24]. Over the span of a structure's life, corrosion progresses gradually and may require several years to cause damage. Penttala [25] found that the surface may undergo degradation for a period of up to 10 years from the initiation of damage to the reinforcement. Hence, several technologies are being devised to accelerate the rusting process. An expedited electro chemical induced corrosion examination will be conducted for this investigation.

Some studies have shown that GGBS can significantly enhance resistance to chloride penetration and mitigate the corrosion of reinforcing steel in aggressive environments. For instance, Siddique and Khan [26] demonstrated that concrete with GGBS exhibits lower chloride permeability due to its refined pore structure, which reduces the ingress of aggressive ions. This improvement is attributed to the pozzolanic reaction of GGBS with calcium hydroxide, resulting in additional C-S-H gel formation that densifies the matrix.

Similarly, Matthes et al. [27] reported that incorporating GGBS into concrete significantly improves resistance to chloride penetration in reinforced concrete. This improvement is attributed to the reduced permeability and denser microstructure of GGBFS-modified concrete, which

limits chloride ion ingress and delays reinforcement corrosion, a critical factor in the durability of concrete structures exposed to marine environments. Additionally, the alkalinity of concrete containing GGBS remains sufficient to protect the steel from corrosion despite the lower calcium hydroxide content. while, Arash and Morteza [28] investigated the impact of GGBS on pavement durability. The results indicated that the cracking, porosity, and permeability characteristics of concrete exhibited a negative correlation with the incremental addition of slag.

Another investigation by Thomas et al. [29] highlighted that GGBS improves the corrosion resistance of steel reinforcement by delaying the onset of corrosion. The authors noted that GGBS-blended concrete exhibited a prolonged time to corrosion initiation under accelerated chloride exposure tests. The enhanced performance was attributed to the lower chloride-binding capacity and higher threshold chloride concentration in GGBS concrete compared to ordinary Portland cement concrete.

Moreover, studies by Burnell and Black [30] emphasized the sustainability and economic advantages of supplementery cementicious materails, suggesting that its incorporation not only improves durability but also reduces the cement content and overall carbon footprint. The authors found that substituting 40% of cement with pulverized fuel ash resulted in decrease in eCO2/MPa within the desired strength range of 50 to 70 MPa.

Babalola et al. [31] studied the concrete mechanical properties and durability using GGBS. They found that the mechanical properties, durability and chloride permeability were superior when the GGBS content was 30%. Reddy S. and Srinivasa.[32] investigated the optimum use of micro silica and GGBS for the strength properties of concrete. Results indicated that the inclusion of GGBS in concrete enhanced both its workability and strength.

Based on the review of existing literature, limited studies have explored the enhancement of concrete properties, particularly corrosion resistance and resistance to chloride ion penetration, through the replacement of cement with a substantial proportion of ground granulated blast furnace slag (GGBS). While prior research has highlighted the benefits of GGBS in improving durability and mitigating the ingress of aggressive agents, the optimal balance between concrete strength, corrosion resistance, and environmental impact remains underexplored. Most existing studies focus on conventional replacement ratios and fail to provide comprehensive insights into achieving the highest corrosion resistance while maintaining adequate structural performance.

This gap underscores the need for a more detailed investigation into the use of high replacement ratios of GGBS in concrete production. The primary objective of this study is to evaluate the performance of concrete mixes incorporating a significant proportion of GGBS. The research aims to determine the optimal design that meets the required strength criteria, offers superior corrosion resistance, minimizes chloride ion penetration, and achieves the lowest environmental impact (EI). By doing so, the study seeks to provide an effective solution for reducing cement consumption, thereby addressing both durability and sustainability concerns in modern concrete applications.

2. THE PROGRAM OF EXPERIMENTAL

2.1. Primary Materials Used

2.1.1. Binders

The binding substances utilized in this work were Ordinary Portland cement (OPC) according to EN BS 197-1:2011[33], and GGBS, which stands for granulated blast furnace slag, as specified in BS EN 15167-1:2006[34]. Laboratory tests have been conducted to assess the physical and mechanical characteristics of these binders according to BS EN standards. Detailed results are presented in Tables 1 and 2.

Table1. Physical and Mechanical Characteristics of Binder Materials

	Specific gravity	Fineness cm^2/g	Consistency (%)	Setting time min.		Strength MPa	
				Initial	Final	2 days	28 days
Cement	3.15	3460	31	106	170	18.4	43.75
GGBS	2.9	4150	-	-	-	-	-

Table2. Chemical analysis of Cement and GGBS

	CaO	SiO_2	Al_2O_3	Fe_2O_3	MgO	K_2O	Na_2O	SO_3	L.O.I
Cement	62.43	19.36	4.82	3.28	3	0.56	0.29	2.26	1.69
GGBS	41.95	35.59	14.32	0.35	7.41	---	---	0.09	0.66

The specific surface area fineness of GGBS was measured to be 4150 cm^2/g, which is greater than the fineness of OPC calculated to be 3460 cm^2/g. An essential Influential factor on the reactivity of GGBS and the early strength growth of concrete is the particle size of GGBS [35]. According to Swamy[36], increasing the fineness of GGBS to two-three times that of cement provides numerous advantages for the engineering characteristics of concrete, including durability, setting time, evolution heat, and bleeding. To achieve optimal efficiency, the surface area of GGBS should fall within the range of 4000 and 6000 cm^2/g [37]. The surface area of the currently utilised GGBS falls within the specified range. The chemical characteristics of the binders were determined by empirical testing and are illustrated in Table 3. Chemical Analysis of the binders reveals that the lime (CaO) content in GGBS (41.95%) is lower than that of cement (62.43%). Nevertheless, the silica (SiO_2) percentage of GGBS (35.59%) and alumina (Al_2O_3) content (14.32%) are higher than cement (19.36% and 4.82%, respectively), therefore guaranteeing its pozzolanic properties. Prior investigations [27,29,30,31] have shown that GGBS mostly exhibit hydraulic activity, which is a cementitious characteristic, together with specific pozzolanic activity. The GGBS material can exhibit cementitious characteristics when combined with activators such as lime, Portland cement, and alkalis including sodium carbonate or sulfate, calcium, or magnesium. The hydraulic activity of GGBS is mostly determined by its producing method and chemical compositions. ASTM C 989-06[40] suggests using the slag activity index as the main evaluation criterion to determine the relative cementitious capacity of GGBS. Therefore, GGBS is categorized into 80, 100, and 120 according to their slag activity indices.

Table 3. Index of slag activity as per ASTM C 989-06

Examination	Grade			GGBS utilized in research
	80	100	120	
7 d	--	75	95	--
28 d	75	95	115	122

Table 3 demonstrates that the GGBS employed in this context meets the criteria of grade 120, particularly having a high slag activity index. The grain gradation of the cement and GGBS used is depicted in Figure 2.

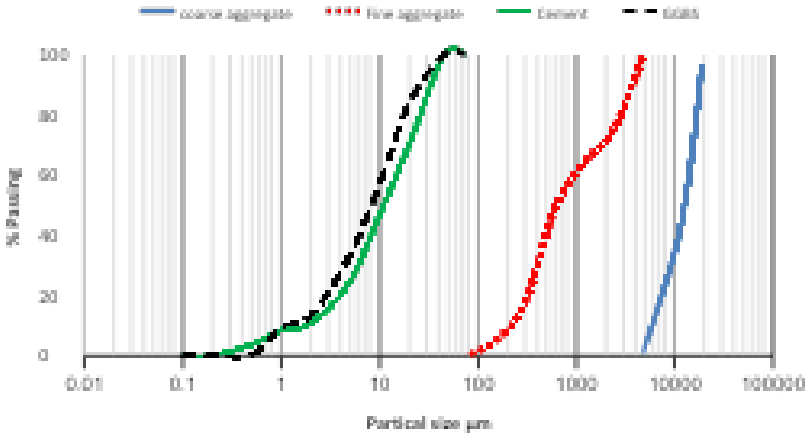

Figure 2. Particle size distribution of cement, GGBS, fine aggregate (FA) and coarse aggregates (CA)

2.1.2. Aggregate

The sources of sand and gravel used in this study are local in Iraq and they are satisfied BS EN 12620:2002+A1:2008 [41] The local sand utilized has a density of 1660 kg/m^3, fineness modulus of 2.91, specific gravity of 2.65 and absorption of water 0.93%. The gravel utilized was crushed, with an upper limit of 19 mm in aggregate size, 1640 kg/m^3 density, specific gravity and absorption of water 2.58 and 0.47%, accordingly. Figure 2 illustrates the granularity gradation of the aggregate utilized.

2.1.3. Superplasticiser

All concrete mixes incorporated high-range water-reducing chemical additives. Its name is Fosroc Structuro W420. It meets the requirements of ASTM C494: 2011[42]. the liquid was distinguished by its light yellow hue, Specific gravity(s.g) 1.04 @ 25°C. The usual dosage range is 0.20 - 2.0 litre/100 kg of cementitious material. In current study, it is used a dose of 0.85% by weight of cementitious material.

2.2. Mixture Proportions

The primary goal of the work was to assess the impacts of GGBS produced during iron ore manufacturing on the mechanicals characteristics, chloride migration, and corrosion resistance of concrete, two concrete mixtures were used as reference mixes with targeted 28d strength of 30 MPa (C30) and 40 MPa (C40) were designed according to the American Standard ACI 211.1 , in addition to use six other mixes containing different ratios of GGBS replacement represented by (30, 40, 50)% of cement weight and were defined as (C30-0%GGBS, C30-30%GGBS, C30-40%GGBS, C3030-50%GGBS, C40-0%GGBS, C40-30%GGBS, C40-40%GGBS, and C40-50%GGBS). Two water-cement ratios were taken for concrete C30 and C40 MPa, which are (0.5, 0.42) % for all replacement ratios. In order to achieve high workability concrete without compromising strength, a superplasticizer additive mixture containing 0.85-1% of cementitious materials was included in all mixes. The desired strength was set at 30 and 40 MPa. The concrete mixing ratios are summarized in Table 4.

Table 4. Mix proportion of concrete mixture

Mixes		Quantities of mixture ingredients kg/m^3					
	Cement %	Cement	GGBS	Fine aggregate	Coarse aggregate	w/b* %	Super plasticizer %
C30-0%GGBS	100	375	---	750	1000	0.5	0.85
C30-30%GGBS	70	262.5	112.5	750	1000	0.5	0.85
C30-40%GGBS	60	225	150	750	1000	0.5	0.85
C30-50%GGBS	50	187.5	187.5	750	1000	0.5	0.85
C40-0%GGBS	100	450	---	680	1000	0.42	1
C40-30%GGBS	70	315	135	680	1000	0.42	1
C40-40%GGBS	60	270	180	680	1000	0.42	1
C40-50%GGBS	50	225	225	680	1000	0.42	1

w/b: Water to binder ratio, GGBS: Ground Granulated Furnace Slug

2.3. The Process of Mixing, Specimens Preparation, and Curing

After preparing the required materials for the concrete mixture, the coarse and refined raw materials (sand and crushed gravel) are mixed in the mixer for one minute. A (250-300 kg) pan-type mixer mixes the concrete components. This step ensures uniform distribution of the raw materials before adding the other components. After that, 50% of the required mixing water is incorporated with the raw materials and mixed for another minute. The purpose of this step is to hydrate the raw materials and achieve initial hydration. Once the water and raw materials are mixed, cement and GGBS are added to the mixer. The mixer runs for one minute to mix the cement materials well with the wet raw materials. This step ensures uniform distribution of cement and GGBS throughout the mixture. After that, Superplasticiser (a chemical admixture used to improve workability) and the remaining water are added to the mixer. Superplasticizer helps in achieving the required fluidity or workability of the concrete. The mixer is operated for 1 minute to ensure proper dispersion of the superplasticizer and uniform mixing of all the components. As shown in Figure 3(a), tight plastic moulds form the concrete sample. The inner surfaces of the molds are lubricated with oil to inhibit adhesion of the concrete to them after hardening. The mixture is placed into the molds, and the samples are then compacted using an electric vibrating device to remove any gaps or voids in the mixture. This ensures proper compaction and eliminates air pockets. In this experiment, different samples are cast using specific moulds, cubes, cylinders and prisms. After 24 hours of casting, the molds are taken out illustrated in Figure 3 (b) and all the specimens are placed in water tanks and dried at room temperature 28 days exemplified in Figure 3(c).

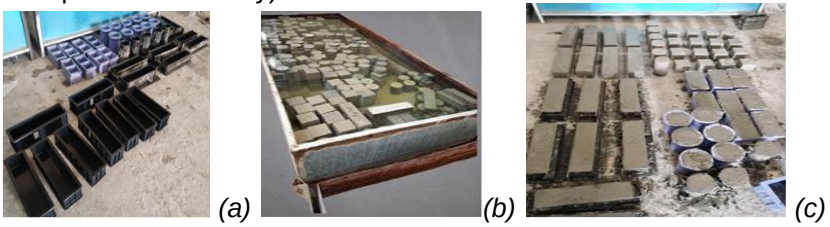

(a) *(b)* *(c)*

Figure 3. (a) the prepared samples, (b) plastic mold and (c)curing

2.4. Testing procedures

In this study, several laboratory tests were conducted and are shown in the following sections.

2.4.1. Fresh Tests (Initial and Final Setting Times and Workability)

According to EN BS 12350-2:2009[43] a slump examination was conducted to assess the workability of all mixes shown in Figure 4(a)., while the Vicat device was utilized to perform initial setting time and final setting time tests for all mixes as shown in Figure 4(b) according to BS EN 196-3:2005[44].

(a)

(b)

Figure 4. (a) slump test (b) Vicat apparatus

2.4.2. Test of Hardened Properties

2.4.2.1. Examination of Compressive Strength

As per BS EN 12390-3:2019[45], the compressive strength examination was performed, a hydraulic compression device (2000) kN was used to test cubes (10 * 10* 10) cm. An average of three cubes is introduced on each check and examined at 28, 56 and 90 days.

2.4.2.2. Splitting Tensile Strength

The examination employed cylindrical molds measuring 10 cm by 20 cm. According to EN BS 12390-6:2009[46]. For all mixes, an average of three cubes is introduced on each check and examined at 28, and 90 days.

2.4.2.3. Examination of Flexural Strength

The present study involved the execution of flexural strength tests on prism specimens with measurements of 10*10 * 40 cm at days 28 and 90. according to EN BS 12390-5:2009[47]

2.4.2.4. Bulk Density

The experiment was conducted using the identical cubes used in the compression test, during which the cubes were weighed and their precise dimensions were verified. Furthermore, the bulk density was determined by dividing the mass of each cubic unit by its size. Three readings were obtained for each outcome.

2.4.3. Tests of Durability Properties

2.4.3.1. Water Absorption and Porosity

According to ASTM C642:2013[48]. The concrete samples utilized in this study underwent porosity and total water absorption tests after 28 and 90 days after initial curing in water. For every combination, three specimens with (10*10*10) cm^3 were prepared. The total water absorption and porosity were determined using the following equation:

$$Total\ water\ absorption=m2\text{-}m1m1*100 \quad (1)$$

$$Porosity=\ m2\text{-}m1m2\text{-}m3*100 \quad (2)$$

where: m_1: represents the dry mass, m_2: saturated mass, m_3: represents the mass of the sample immersed in water

2.4.3.2. Microscopic Analysis of the Structure

For this examination, small concrete samples of approximately 5*5 mm dimensions were taken from the reference mix samples and from the samples in which cement was substituted with GGBS. A scanning electron microscope (SEM) was used for this purpose. Before the examination, the specimen was dehydrated in an oven set at 110 °C for 24 hour. Subsequently, its surface was polished by applying a diamond polish. A thin layer of copper was coated on the sample to make it electrically charged, and then the sample was placed on the SEM stem.

2.4.3.3. Examination of Electrical Resistivity:

Electrical resistivity measurement is a criterion the classification of concrete based on its corrosion rate. Utilizing the direct two electrode technique necessitates access to both sides of the concrete. Given a steady voltage, the current flowing through the concrete is measured and documented. To get the resistance (R) of the concrete, the following equation is used:

$$R=VI \quad (3)$$

where:

V: represents the applied voltage, and I represents the electric current flowing through sample.

The following equation was used to determine the concrete's resistivity[49]:

$$q=Rat \quad .(4)$$

where:

q represent the electrical resistivity of the concrete, measured in kΩ. cm, electrical resistance is denoted as R,

A represents The sample's surface area, and height of sample is denoted by t.

An electrical resistivity examination of concrete was conducted using the commercially available direct two electrode method. The concrete specimens used for testing had dimensions of

(10*10*10) cm^3. The concrete sample was positioned between two plates, a wet sponge was inserted to ensure electrical conductivity. The average of three readings was recorded for each result.

2.4.3.4. Rapid Chloride Migration Examination

Using the non-steady state migration test specified in NT Build 492:1992 [50], the resistance against chloride ingress of concrete samples was evaluated to calculate the chloride migration coefficient. The procedure involves applying an external electric field to a concrete specimen of 100 × 50 mm, which induces the migration of chloride ions into the specimen. Once the specimen has been split, the chloride penetration is quantified by the spraying of a silver nitrate onto the divided portions. On the basis of the penetration depth, the non-steady state migration coefficient is computed. Figure 5 depicts the experimental arrangement and the specimens utilized for testing subsequent to the application of the silver nitrate. The migration coefficient was consequently computed using Equation (5):

$$D_{nssm} = 0 \cdot 0239273+T*LU-2*t(Xd - 0 \cdot 0238273+ +T*L*XdU-2)5$$

where: D_{nssm}: coefficient of non-steady state diffusion m^2/s, T: is the mean value of the beginning and final temperatures solution at the anode, measured in $^oC.$, L: represents the sample thickness in millimemeters, U: the absolute value of the voltage that is being applied (V), Xd: represents the mean value of the penetration depths in millimetres, and t: the length of the examination (in hours).

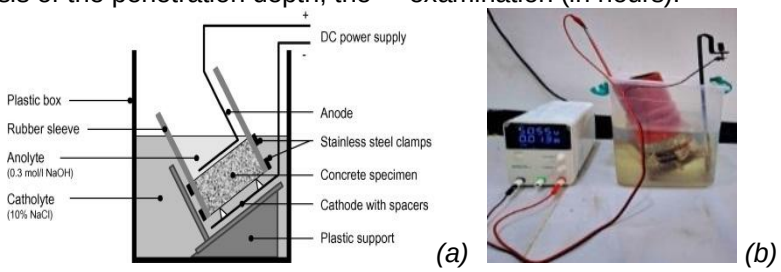

Figure 5.Experimental arrangement for the Rapid Chloride Migration test (a) schematic depiction (b) Implementation of the conducted tests

2.4.3.5. Corrosion Rate by Impressed Current Test (IC):

The corrosion of steel is slow. Alkaline concrete takes slower to corrode, even under harsh conditions. Due to the time required to replicate reinforcement corrosion in labs, accelerated corrosion test procedures have been developed. Impressed current is a fast and effective accelerated corrosion test method that decreases de-passivation corrosion initiation time from years to days.[51]. In this method, a continuous direct current (DC) is applied to the embedded steel in the concrete to initiate corrosion. The current is impressed from the electrode to the reinforcement through concrete immersed in an electrolyte (sodium chloride solution) [52]. This research used prismatic specimens with dimensions of (10*10*20) cm. Steel bars of 15 cm length were prepared and weighed. This weight measurement serves as a reference for evaluating mass loss due to corrosion. In addition, the rebar were connected with copper wires. The steel bars were inserted into the prismatic mold with a 2 cm cover. The concrete pouring process was carried out smoothly. After 24 hr., the samples were unmolded and subjected to a 28-day curing process. After hardening, the specimen were placed in a 5% NaCl solution. At the bottom of the sample, a stainless steel mesh was placed connected to the wires and connected to the DC power source, representing the cathode electrode. As for the electrical wires in the sample, a 1 kΩ variable resistance was placed in them and connected to the power source as an anode electrode. Then the current was applied while maintaining the voltage constant as shown in Figure 6. The period was 26 days, calculated by Faraday's law to achieve 10% corrosion as shown in Equation 6. After this period, the samples were divided into two halves, the steel was removed, cleaned, and weighed.

$$t=m*z*FM*I \qquad .(6)$$

where: t: represents the time in second, m: represents the mass loss in gram, Z: valance (2), F: represents the Faradays constant equal to 96480 (in A.sec.), M: The atomic weight of the metal is 55.85, I: represents the Imposed current in ampere.

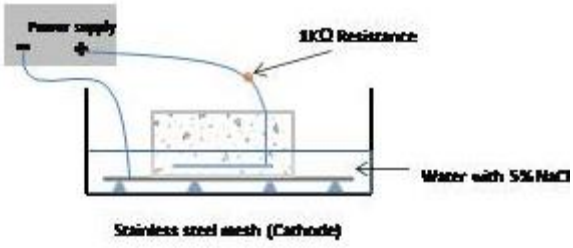

Figure 6. Impress current test

2.4.3.6. Analysis of Environmental Impact (EI)

The environmental impact of the mixes proposed in this work is examined by assessing the collective influence of concrete ingredients such as Cement, sand, gravel, GGBS, and water on various environmental factors. Abiotic depletion potential (ADP), global warming potential (GWP), photochemical ozone generation potential (POCP), acidification potential (AP), and eutrophication potential (EP) are the several environmental factors taken into count. The literature was consulted to gather data on the environmental effects of each component in producing of 1 m^3 concrete. The findings are summarized in Table 5. Concrete utilizing GGBS is subjected to an environmental impact study using the inventory data provided in Table 5. This environmental impact analysis considers all eight concrete mixes, including the reference mixes. Calculations were performed to determine the effects of six concrete mixes in terms of the percentage reduction compared to the reference mix on various environmental factors.

Table 5. Environmental effect data for producing of concrete constituent

Material	Reference	ADP	GWP	POCP	AP	EP
		kg Sbeq	kg CO_2eq	kg C2H4eq	kg SO2eq	kg PO4eq
Cement (1 kg)	Kurda et al.(2018)[53]	3.83×10^{-3}	9.27×10^{-1}	7.52×10^{-5}	2.55×10^{-3}	3.50×10^{-4}
Sand (1kg)		3.30×10^{-10}	9.87×10^{-3}	2.80×10^{-6}	4.58×10^{-5}	1.08×10^{-5}
Gravel (1kg)		1.09×10^{-9}	2.44×10^{-2}	7.83×10^{-6}	1.44×10^{-4}	3.18×10^{-05}
GGBS (1 kg)	Kim et al.(2016)[54]	4.55×10^{-5}	5.19×10^{-2}	1.29×10^{-5}	1.72×10^{-4}	6.38×10-5
Water (1kg)	Kurda et al.(2018)[53]	1.57×10^{-11}	1.33×10-4	4.99×10^{-8}	3.87×10^{-8}	9.70×10^{-7}

3. RESULTS AND DISCUSSION

3.1. Fresh Examination Results

3.1.1. Slump

In Fig.7, it is evident that the concrete using GGBS has enhanced workability in comparison to the reference mixture. Moreover, when the substitution percentage rises, there is a clear and substantial improvement in workability. Findings of this investigation are basically in line with the earlier results [47,48]. It is clear that the increase in the slump value of the C30 mixes (C30-30%GGBS, C30-40%GGBS, and C30-50%GGBS) was (10, 20, 25)% respectively, compared to the reference mix, which had a slump value of 100 mm. The increase in C40 mixtures (C40-30%GGBS, C40-40%GGBS, and C40-50%GGBS) was (4.16, 8.3, and 12.5)%, respectively, compared to the reference mix (C40-0%GGBS), which had a slump value of 120 mm. The enhanced workability of concrete including GGBS can be ascribed to the greater dispersion of cement particles and the surface characteristics of the GGBS, which display a smooth surface (vitreous phase) and high density, resulting in less water absorption during mixing. [49,50,51].

3.1.2. Results of Initial and Final Setting Time

As shown in Figure 8, when OPC was replaced by 30%, 40% and 50% of the cement weight with GGBS, the initial setting times were slightly prolonged by (3, 7, and 21) min respectively, compared with reference. the final setting times rose from 170 min for the reference mix to (176, 180 and 185) min with the mixtures containing GGBS at replacement ratios (30%, 40% and 50%), respectively. The slightly prolonged setting time facilitated the transportation, placing and compaction of concrete prepared with these blended cement. The observed increases due to the prolongation of the hydration process of GGBS and a reduced amount of OPC [60]. Similar results were with previous findings[53,54].

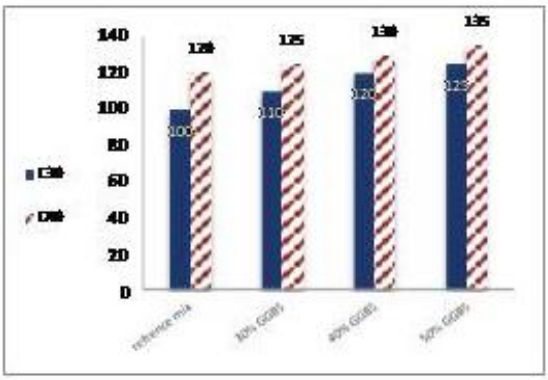

Figure 7. Results of the slump test

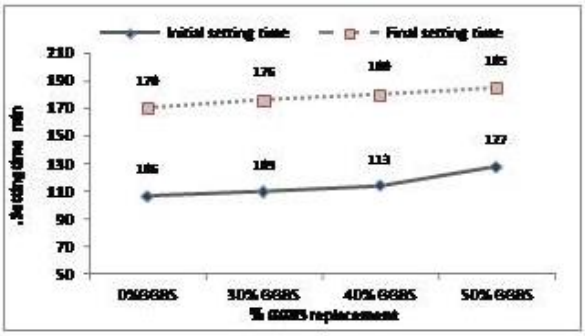

Figure 8.Represents results of initial and final setting time

3.2. Hardened Examination Results

3.2.1. Results of Compressive Strength

The compression examination results for all mixtures (with and without GGBS) at 28, 56, and 90 days are presented in Figure 9. Evidently, compressive strength of the mixtures rises as the curing age progresses, owing to the production of more C-S-H as a hydration of cement result and improvement of the microstructure of concrete [63]. It was discovered that the introduction of GGBS in concrete mixes at (30, 40 and 50)% of cement weight enhances the compressive strength over all test ages, and this increase is gradual with increasing replacement ratio up to 40% after which the compressive strength starts to decrease slightly at 50% replacement ratio. These results indicate a continuous and significant contribution of GGBS to the compressive strength in comparison to the reference concrete mix (0% GGBS). At 28 days, the compressive strength of the mixes (C30-30%GGBS, C30-40%GGBS, and C30-50%GGBS) improved by (10.4-36.3) % compared to the reference mix (C30-0%GGBS), and at 56 days it ranged between (14.8% and 34.3%), while the compressive strength at 90 days recorded (44, 50, and 49.27) MPa, respectively. As for the mixes (C40-30%GGBS, C40-40%GGBS, and C40-50%GGBS), the percentage improvement in compressive strength was between (5.97-17.14)% at 28 days, and at 56 days it was between (8.27, and 19.37)%, while at 90 days the compressive strength recorded values (51.2, 56, and 53.23) MPa respectively. The concrete mix (C30-40%GBS and C40-40%GGBS) gave the highest values for all ages. The enhanced strength is ascribed to the pozzolanic interaction between GGBS and cement, which exhibits greater stability with ageing [64]. This trend was in agreement with previous studies[56,47,24,21].

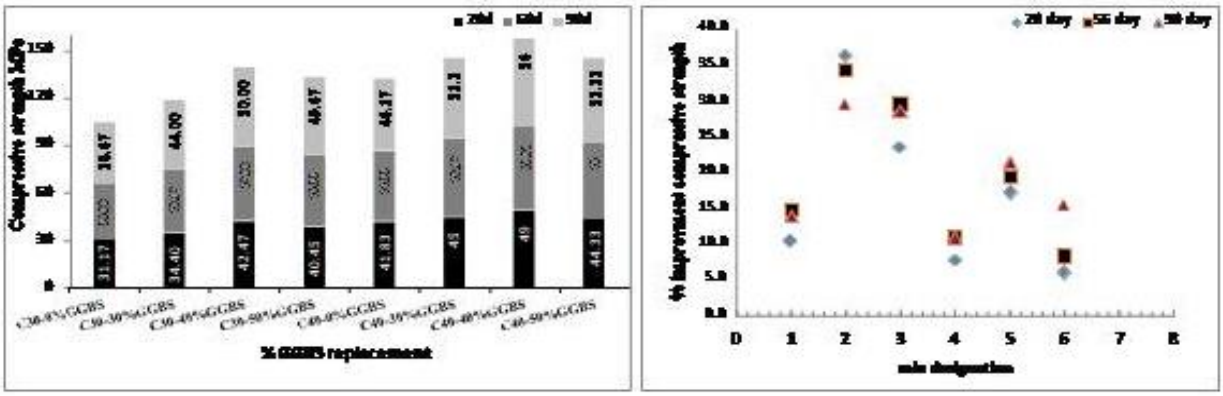

(a) *(b)*

Figure 9. (a)compressive strength results for (28 , 56 and 90) days (b) Enhancement in Compressive Strength of with the addition of GGBS at 28, 56, and 90 days

3.2.2. Splitting Tensile Strength

In this test, results were evaluated after 28 and 90 days of curing. The experimental findings are summarized in Figure 10. The relation between splitting tensile strength and GGBS amount exhibited a similar pattern to the observed trend in compressive strength. The splitting tensile strength exhibited a positive correlation with the GGBS content at all stages of development. The reference mixes (C30-0%GBS, C40-0%GGBS) recorded indirect tensile strengths of (2.95 and 3.52) MPa at 28 days and (3.62 and 4.3) MPa at 90 days. The tests revealed that the split tensile strength of the mixtures (C30-30%GGBS, C30-40%GGBS, C3-50%GGBS) increased by a range of 4-15.3% at 28 days and 20-38.7% at 90 days. The mixtures (C40-30%GGBS, C40-40%GGBS, C4-50%GGBS) recorded an increase of (12.8-26.1)% at 28 days and (11.5-19.2)% at 90 days, respectively, comparison to the reference mixtures. The mixtures (C30-40%GGBS and C40-40%GGBS) had the most significant improvement in splitting strength, which was (15.3 and 26.1) at 28 days and (38.7 and 19.2) at 90 days, sequent. Enhancement in strength is attributed to enhanced bonding of mineral admixtures (GGBS) with cement and Other components of concrete [65]. Reddy et. al. [66] have found that incorporating ultra-fine particles of GGBS into concrete improves packing density and promotes the connecting and binding of component parts. Thus, strength improvement is noticed. These results are consistent with previous work[24,22].

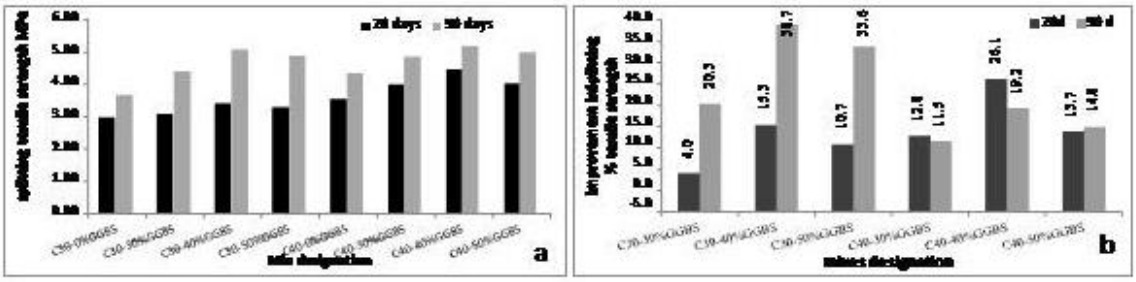

Figure 10. (a) Splitting Tensile Strength values : (b) Improvement in Splitting Tensile Strength values for 28 and 90 days

3.2.3. Results of Flexural Strength

Figure 11 displays the resulting flexural strength values at 28 and 90 days for mixes of concrete (C30, C40) including varying ratio of GGBS. This figure shows that flexural and compressive strength behave similarly. All mixtures have higher flexural strengths than the reference mixture. These values increase with increasing partial replacement of GGBS compared to the reference mixture (without GGBS), where mixtures (C30-40%GGBS, and C40-40%GGBS) obtained the highest flexural strength values (5.9, 6.3) MPa at 28 days and (6.73, 6.99) MPa at 90 days respectively, after which there was a slight decrease in flexural strength at 50%GGBS replacement ratio. The mixtures (C30-30%GGBS, C30-40%GGBS, and C30-50%GGBS) recorded an increase in flexural strength at ages 28 and 90 days, ranging between (7-16.6)% and (6.2-15.8)% in comparison to the reference mixture, respectively, while the increase in the mixtures (C40-30%GGBS, C40-40%GGBS, and C40-50%GGBS) reached (3.7-16.3) and (5.3-16.2)% at 28 and 90 days, sequent, in comparison to the reference mix. The improvement in this property is primarily due to the enhanced bonding between the paste and the aggregate and the reduced porosity in the matrix. These results were consistent with the study[57,56].

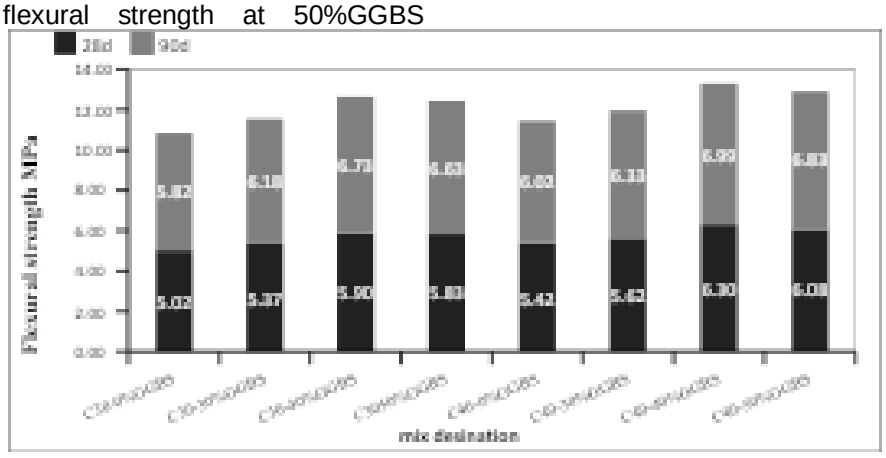

Figure 11. Flexural strength values at (28 and 90) days

3.2.4. Bulk Density of Concrete:

The concrete density examination was conducted at 28 and 90 days for all mixes (with and without GGBS), illustrated in Figure 12. The findings demonstrated a reduction in density by the incorporation of 30%, 40%, and 50% of GGBS by weight of cement, as the mixes (C30-30%GGBS, C30-40%GGBS, and C30-50%GGBS) achieved value are range between (2343.3 to 2360) and (2346.6 to 2370) kg/m^3 at 28 and 90 days in order manner, less density compared with the reference mix (C30-0%GGBS). As for the mixtures (C40-30%GGBS, C40-40%GGBS, and C40-50%GGBS) achieve Density ranging between (2325 to 2342) kg/m^3 and (2363, 2344.6) kg/m^3 in comparison to reference mixture at 28, and 90 days in order manner. The findings show that the density reduces as the proportion of cement substituted by GGBS rises. The observed decrease in density was resulted from the greater specific gravity of cement in comparison to GGBS. Moreover, the decrease can also be ascribed to the fact that, similar to other supplementary cementitious materials (SCMs), GGBS initially functions as a

filler and needs to wait for the activation of $Ca(OH)_2$ generated during the hydration process before the pozzolanic reaction can take place. In essence, the decrease in density over time is caused by the depletion of $Ca(OH)_2$ during secondary hydration, leading to the formation of less dense calcium silicate hydrate compared to the cement constituents from which $Ca(OH)_2$ is derived[67]. This observation is similar to that of Bheel N. et al. [68].

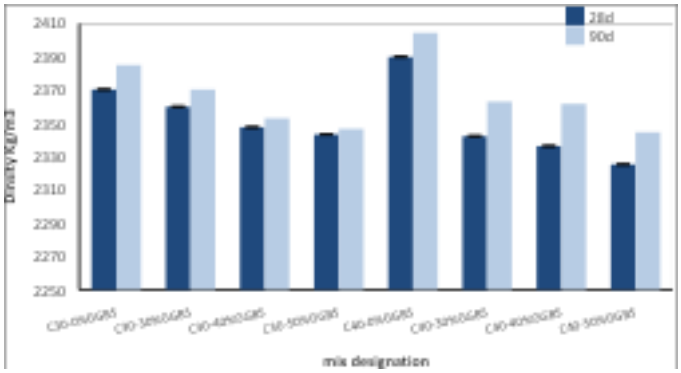

Figure 12.Density of concrete specimens at 28 and 90 days.

3.3. Durability Examination Results

3.3.1. Porosity

Figure 13 illustrates the result of concrete porosity with GBBS substitutes carried out at 28 and 90 days. Evidently, with rising percentage of GGBS substitution, the porosity of concrete reduces. Reduce in porosity is ascribed to the pozzolanic reaction with cementitious secondary materials (C-S-H), which enhanced the mortar binding property, leading to lower permeability. Moreover, the partial filling impact of GGBS, which fills the empty spaces in the aggregate, results to a denser mass, at last decreasing the porosity of the concrete. The porosity of concrete is directly enhanced by the synergistic interaction of pozzolanic and micro-void filling.

At 90 days, the highest porosity measured was (7.32)% at C30-0% GGBS, while the minimum porosity measured was (3.42)% for C30-50% GGBS. As for the second group mixes (C40), the behaviour was similar to the first group mixes, as The maximum porosity was determined to be (7.15)% with C40-0% GGBS. In comparison, the minimum porosity was calculated to be (2.47) % with C40-50%GGBS at 90 days. Furthermore, the porosity of concrete is an essential factor. Among the characteristics of durable concrete, concrete with low depth of water penetration shows excellent resistance to chemical attacks [15].

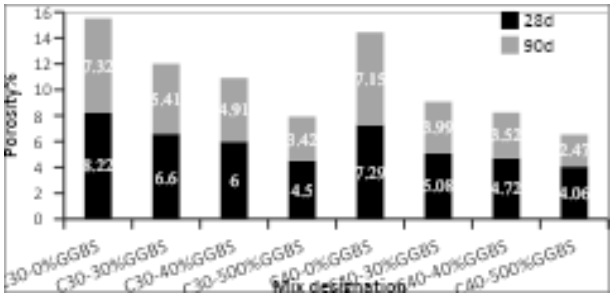

Figure 13. Results of porosity tests conducted at 28 and 90 days

3.3.2. Results of Water Absorption

Figure 14 presents that absorption of water of the concrete mixes (C30-30%GGBS, C30-40%GGBS, C30-50%GGBS) decreased significantly by about (49.0, 54.2, 61.8) %, and (45.1, 49.3, 68.8) %, respectively at 28 and 90 days, in comparison to the reference mix (C30-0%GGBS). While the water absorption of the second series mixtures (C40-30%GGBS, C40-40%GGBS, and C40-50%GGBS) also recorded a significant decrease, as shown in the following figure, and was (49.60, 55.437, 59.94) %, and (53.01, 55.87, 66.6) % at 28 and 90 days, sequent, when contrasted to the reference mixture (C40-0%GGBS). It can be noted that with age progress and increased GGBS content, water absorption decreases; decreased absorption of water denotes improvement of the microstructure of concrete over time. This finding may be due to the fact that these mixes contain fewer interconnected pores as C-S-H forms from primary hydration and secondary

pozzolanic reactions of GGBS and gradually fills water-filled spaces. In addition, GGBS had high fineness functioning as fillers between cement particles, which might enhance this phenomena [69].

The most significant decrease in water absorption was recorded at 90 days of age for the mixtures C30-50%GGBS and C40-50%GGBS, where its value was (1.09, and 1.05) %, compared to the reference mixtures, whose valueswere (3.49, and 3.15) % respectively. These results conform to the study Aghaeipour and Madhkhan[21,23]

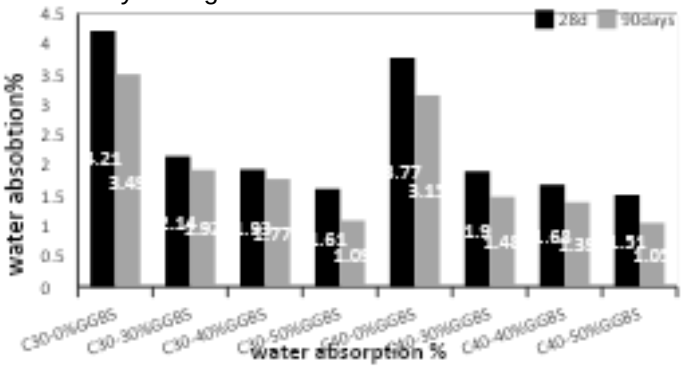

Figure 14. Water absorption behavior of concrete mixtures at various stages of curing

3.3.3 Electrical resistivity

Concrete specimens were subjected to electrical resistance testing at 28 and 90 days of age using the direct two-electrode technique. The relation between corrosion rate and electrical resistance, as determined by the direct two-electrode technique, is presented in Table 6[71].

Table 6 Electrical resistivity EI measurement of the concrete[71]

ER kΩ.cm	Rate of Corrosion
>20	Low
10–20	Low to moderate
5–10	High
<5	Very high

Measurement and categorization of the corrosion rate of concrete mixtures are demonstrated in Figure 15. The electrical resistance is inversely proportional to the corrosion rate, increasing with the percentage of GGBS replacement by the weight of cement. It is clear that the concrete mix containing the highest percentage of GGBS replacement (50%GGBS) recorded a meagre corrosion rate and high electrical resistance at 28 and 90 days for both groups(C30, C40), followed by the mixture with a 40% replacement percentage (40%GGBS), and then the mixture with a replacement percentage of (30% GGBS), where at 90 days, the electrical resistance measurement ranged between (32.57 to 41.63) kΩ.cm for mixes (C30-30%GGBS, C30-40%GGBS, C30-50%GGBS) and (39 to 74.03) kΩ.cm for mixes(C40-30%GGBS, C40-40%GGBS, C40-50%GGBS), compared with the reference mixtures, which recorded values of (10.86) for the mix(C30-0%GGBS) and (15.23) for the mix(C40-0%GGBS), which greatly exceeds the value of 20 (kΩ.cm) given by Table 6 for low-value corrosion rate. Therefore, mix corrosion (40%GGBS) is unlikely to occur after 90 days of curing. The introduction of GGBS and the subsequent pozzolanic reaction cause physical condensation of the microstructure, which in turn stimulates the production of secondary C–S–H bonds. The development of secondary bonds will enhance the resistivity of concrete[72]. To a greater extent, the ions will have a more difficult time moving through the concrete if the electrical resistivity of the concrete is higher. Thus, this inhibits corrosion [73]. This is consistent with what other researchers have found Bhojaraju[74] The relation between concrete resistivity and corrosion rate [71].

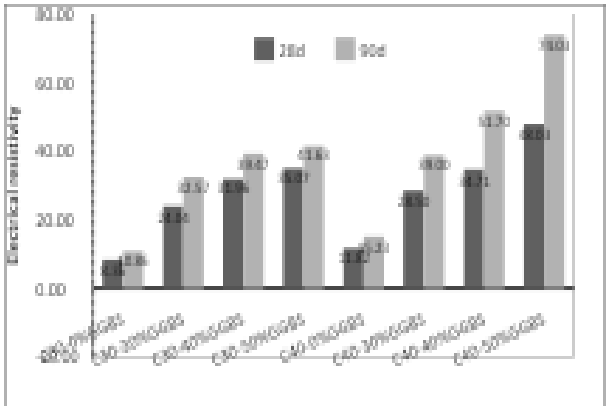

Figure 15. Electrical resistivity test results at 28 and 90 days

3.3.4. Depth of Chloride Ion Penetration

A test was conducted to assess migration at 28 and 90 days of age. The depth of chloride ion penetration was determined by spraying a 0.1 N silver nitrate to the fresh fracture surfaces of the specimen. To ascertain the penetration depth, Figure 16 displays the split face of the concrete specimens that were sprayed with the $AgNO_3$ solution.

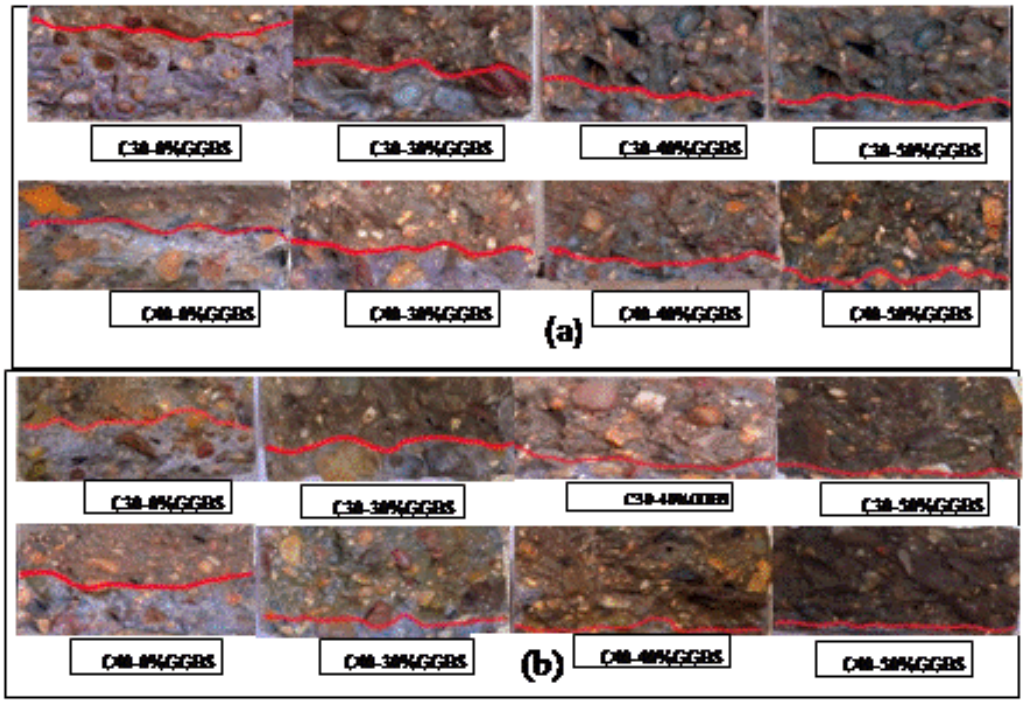

Figure 16. Depth of chloride penetration into concrete mixture with different percentage of GGBS: (a) For 28 days (b) For 90 days

The superficial sections of the mortar samples had a lighter hue as a result of the presence of silver chloride, a white deposit that serves as an indicator of the level of chloride penetration. By contrast, the internal parts of the samples appeared darker due to the formation of silver hydroxide precipitation. Also, the depths of chloride ion penetration into all concrete mixtures are presented in Figure 17.

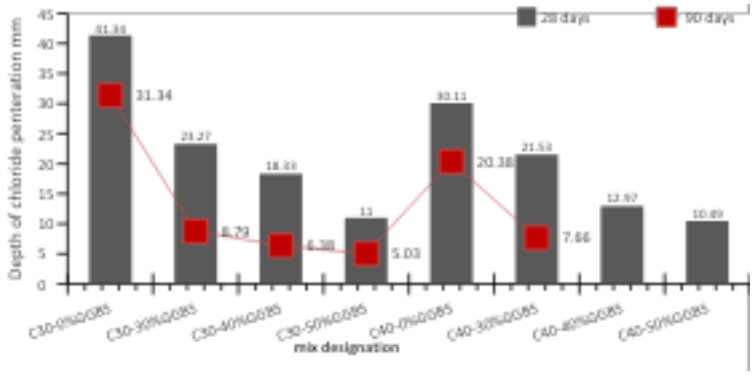

Figure 17. Correlation between chloride penetration depth and GGBS replacement amount at 28 and 90 days

Clearly, the extent of chloride ion penetration reduces as the GGBS replacement ratio rises., and the decrease is more significant with the mixtures of the second series C40, the depths of chloride ion penetration for concrete mixtures including GGBS (C30-30%GGBS, C30-40%GGBS, C30-50% GGBS, C40-30%GGBS, C40-40%GGBS, and C40-50%GGBS) were (23.27, 18.33, 11, 21.53, 12.97, and10.49) mm at 28 days, which was approximately (41.15, 55.2, 75.2, 27.55, 59.6, and 69.6)% lower than that of the C30-0%GGBS and C40-0%GGBS (reference mixture), respectively,

and decreased to (8.79, 6.38, 5.03, 7.66, 4.33 and 3.74) mm at 90 days, which was approximately (76.8, 84.2, 85.9, 64.9, 80.75, and 85.4)% lower than that of the C30-0%GGBS C40-0%GGBS (reference mixture), respectively. The results suggest that higher quantities of GGBS substitution enhanced the concrete's resistance mixture against chloride penetration. chloride penetration into the concrete mixture C40-50%GGBS is almost non-existent. The rise in chloride resistance can be attributed to the physical densification of the pore structure caused by the replacement process of GGBS. Moreover, the high chloride binding capacity of GGBS, due to its significant Al_2O_3 content, as reported by Obada et al.[75] and Yttedal [76], contributes to this increase. GGBS as a binder to replace OPC had an apparent positive influence on durability of mixture in terms of chloride ion penetration resistance. This is consistent with other researchers Natanzi et al. [77].

3.3.5. Non-Steady-State Diffusion Coefficients of Chloride Ions (D_{nssm})

The main factor responsible for steel bar corrosion is chloride ions, which also diminish the lifespan of concrete constructions. The permeability of chloride ions is a crucial variable in assessing the ability of concrete to withstand corrosion caused by chloride. Cracking and spalling of concrete are strongly related to the rebar corrosion, particularly in structures that are exposed to maritime conditions and roadways[78]. The rapid chloride migration coefficient test can assess the resistance to chloride ion penetration of concrete mixture. Hence, the corresponding chloride migration coefficient could determine the chloride migration coefficient at the curing ages of 28 and 90 days, according to Equation 7, and the findings of the analysis are visualised in Fig.18. The chloride migration coefficients at 28 days for the reference mixture and concrete mixture containing different replacement with GGBS (C30-0%GGBS, C30-30%GGBS, C30-40%GGBS, C30-50%GGBS, C40-0%GGBS, C40-30%GGBS, C40-40%GGBS, C40-50%GGBS) were (20.78, 12.23, 9.31, 5.15, 15.57, 11.28, 6.29, and 4.73)*10^{-12} m^2/s, in order manner. At the same time, recorded values at the age of 90 days were (16.55, 3.48, 2.62, 2.34, 9.51, 3.34, 1.83, and 1.39)*10^{-12} m^2/s, respectively. It is noted that adding GGBS to concrete mixtures led to a significant reduce in D_{nssm} in comparison to the mixture without GGBS. The decline in chloride migration coefficients of concrete containing GGBS can be attributed to the pozzolanic interaction with secondary cementitious materials. This interaction enhances the binding characteristics of the mortar, resulting in reduced chloride migration coefficients. Moreover, the filling impact of GGBS, which fills the spaces in the aggregate, results in a more dense mass, ultimately reducing chloride migration coefficients of the concrete [79].This is consistent with other researchers such as Kopecskó and Balázs [80] and Zhao et al.[81].

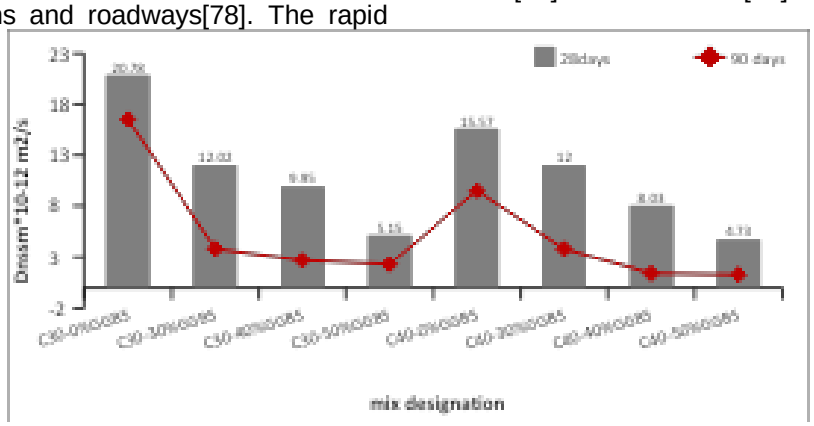

Figure 18. Chloride migration coefficient of concrete mixtures with and without GGBS

3.3.6. Microstructural Analysis

Scanning Electron Micrographs (SEM) examination was conducted on broken small fragments of flexural strength specimens to evaluate the microstructure behaviour of concrete. SEM provides data on the material's topography and compositional characteristics. Small fragments of the specimens were affixed to SEM stub and images were captured using the scanning electron (SE) imaging mode. In Figure 19, scanning electron microscope (SEM) images are displayed for a reference specimen (C30-0%GGBS) and a mixture which includes 50% GGBS (C30-50%GGBS). Figure 19(a) clearly shows that the C30-0%GGBS mixture exhibits cracks and a weak interfacial transition zone after 28 days of curing. Figure 19(b) demonstrates that the visibility of the C-S-H increases for specimens in the C30-50%GGBS range. Nevertheless, the C-S-H that is produced has a porous structure. This suggests that the calcium hydroxide crystals undergo a subsequent pozzolanic reaction, resulting in their conversion into C-S-H. The less homogeneous pattern of C-S-H could be attributed to the partial

interaction of GGBS with water and glossy slag particles during this curing phase. Prolonging the cure period to 90 days, results in a highly compact structure of the C30-50%GGBS mix, characterized by a significant quantity of C-S-H and little pores (Figure 19(c).

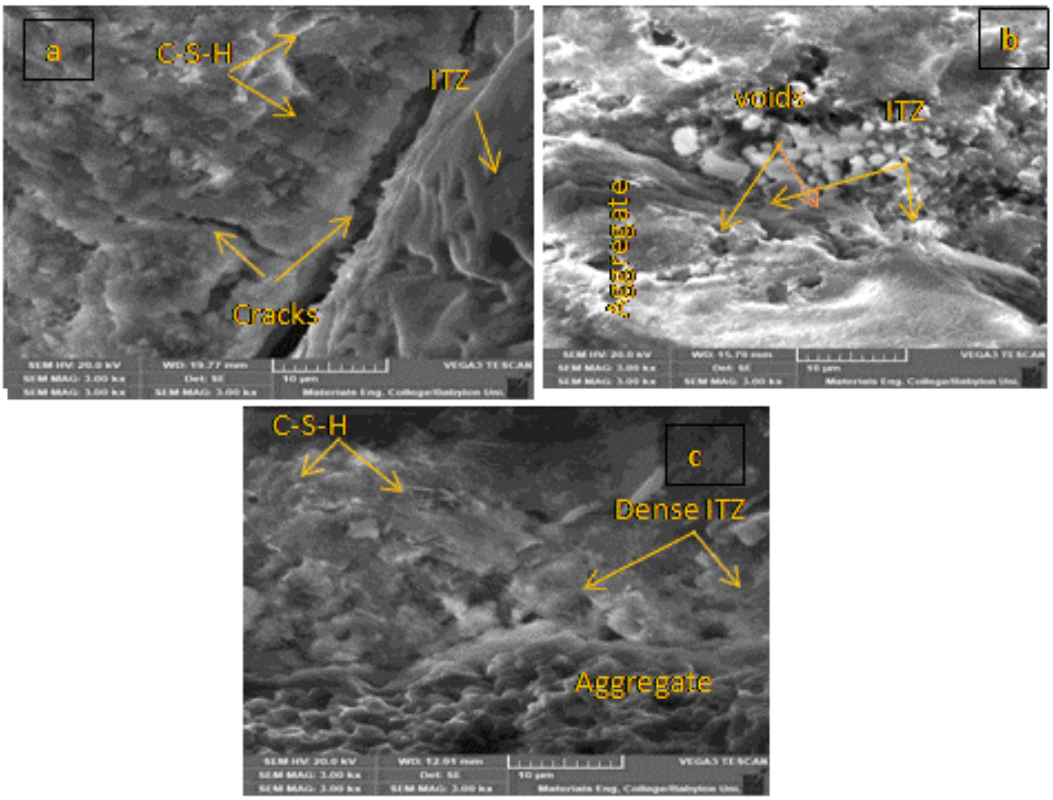

Figure 19. Scanning Electron Morphology of (a) C30-0%GGBS mix at 28 days, (b) C30-50%GGBS mix at 28 days, and (c) C30-50%GGBS mix at 90 days of curing age

3.3.7. Corrosion Rate by Impressed Current Test

After 26 days of subjecting to chloride solution and impress current, the concrete prisms are carefully broken to get out the rebar that is embedded in the concrete without damage; then the rebar is cleaned by using a sandblast machine and stiff metal brush to get out the rust as the showed in Figure 21. The rebar weights are measured and recorded before casting and after sand blast shooting. The gravimetric mass loss and corrosion rate test was conducted by ASTM G1 2003[82] as shown in Equation 7, 8:

$$Mass\ loss = Mi - MfA \quad (gcm2) \qquad (7)$$

$$Corrosion\ Penetration\ Rate\ (CPR) = K*WA*T*D \qquad (8)$$

where: Mi is initially mass in grams, Mf is the final mass in grams, K represents the constant for unit required($8.76*10^4$), W represents the mass Loss in grams, A represents exposed surface area (cm^2), T is exposure time (in hours) and D is alloy density (g/cm^2).

The data in Figure 20 clearly shows that the mass loss and corrosion rate of the steel bar decrease as the GGBS content increases. Furthermore, this decrease is more pronounced as the replacement ratio increases, compared to the mix without GGBS. The mixtures in the second group (C40) exhibit a higher rate of decrease in mass loss and corrosion rate compared to the mixtures in the first group (C30). The mass loss and Corrosion rate for the mixtures (C30-30%GGBS, C30-40%GGBS, C30-50%GGBS, C40-30%GGBS, C40-40%GGBS, and C40-50%GGBS) were approximately between (0.191, 0.063) g/cm^2 and (4.45, 1.316) mm/yr respectively, while for the reference mixtures (C30-0%GGBS, and C40-0%GGBS) it was (0.276, 0.191) g/cm^2 and (6.38, 4.19) mm/yr, respectively.

The concrete mixture containing the highest percentage of replacement with GGBS (C40-50%GGBS) obtained the lowest mass loss and corrosion rate, which was (0.063 gm/cm^2, and 1.31mm/yr) respectively. This decrease in the rate of corrosion and mass loos ascribed to the process of development of a denser microstructure in the concrete due to the presence of GGBS particles.

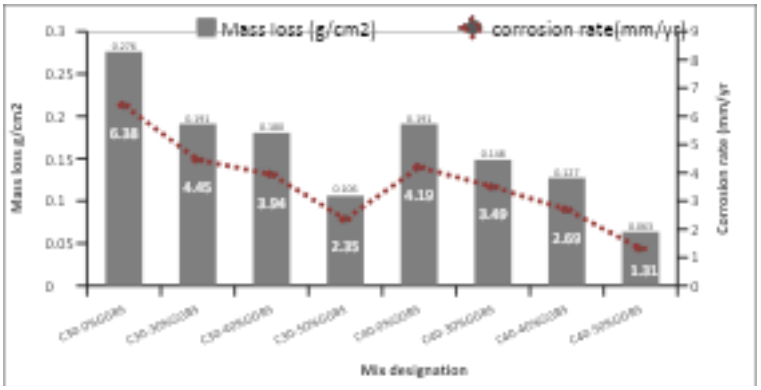

Figure 20. Corrosion rate and mass loss of concrete samples with and without GGBS

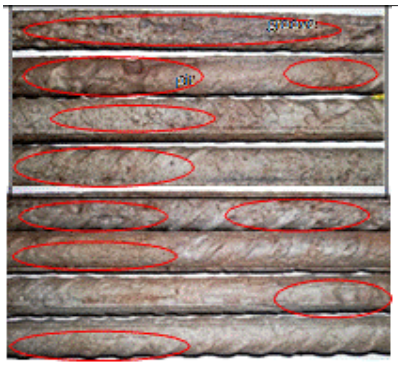

C30-0%GGBS
C30-30%GGBS
C30-40%GGBS
C30-50%GGBS
C40-0%GGBS
C40-30%GGBS
C40-40%GGBS
C40-50%GGBS

Figure 21.Shows the corroded reinforcement steel for all mixes

3.3.8. Cracks Width

During the rebar corrosion process, the volume of corrosion products or rust that can be formed on the rebar surface increases, which generates internal pressure on the surrounding rebar concrete. This increase in internal pressure is more tensile strength capacity of concrete that can cause cracks to form along the face of the concrete parallel to the rebar and cracks on the sides of the area surrounding the rebar, illustrated in Figure 22. From Figure 23, it is clear that the maximum crack width was most prominent in the reference samples without GGBS (C30-0%GGBS), followed by (C40%-0%GGBS), where the crack width was recorded as (0.7, 0.43) mm, respectively. While the crack width seemed to decrease with the inclusion of the mixture with GGBS, the crack width of the mixtures (C30-30%GGBS, C30-40%GGBS, C30-50%GGBS, C40-30%GGBS, C40-40%GGBS, and C40-50%GGBS) ranged between (0.4 and 0.16) mm. The concrete mixture containing the highest percentage of replacement with GGBS (C40-50%GGBS) obtained the lowest crack width (0.16) mm). These cracks might result in a decrease in the durability and strength of the concrete, as well as the potential for further corrosion to occur.

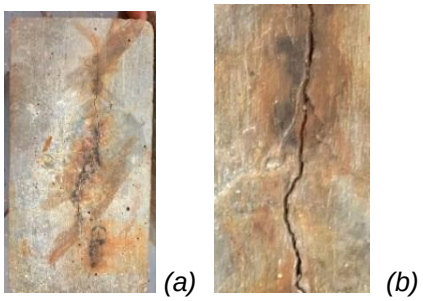

(a) (b)

Figure 22. Illustrates the occurrence of corrosion-induced cracks in the concrete samples, including (a) the rusted specimen and (b) the longitudinal splitting crack that was caused by corrosion

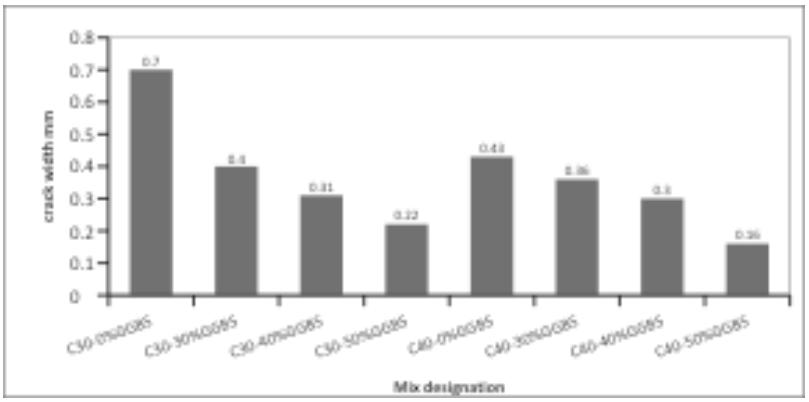

Figure 23. The effect of GGBS content on crack width cause by corrosion

3.3.9. Environmental Impact of Concrete Mixes

The concrete mixture including GGBS is assessed using environmental effect indicators, as depicted in Figure 24(b). global warming potential (GWP), acidification potential (AP), overfeeding potential (EP), non-renewable primary energy input (PEI non-re), and photochemical ozone production potential (POCP) are distinct environmental impact indicators. All pertinent data for each environmental impact indicator is gathered from some references.[83,84,85]. The effects of various concrete mixes were determined by calculating the percentage reduction compared to the effect of the reference mixture on certain environmental factors. The results of this calculation are presented in Figure 24(a). Compared with the reference mixtures (C30-0% GGBS and C40-0% GGBS), the parameters of concrete mixtures containing 50% GGBS replacement are significantly decreased, mainly because of the replacement of cement by a high proportion of GGBS. In addition, compared with the reference mixtures of both grades (C30, C40), about 43.2% of GWP, 39.3% of AP, 31.3% of EP, 30.6% of POCP and 49.4% of PEI non-re are achieved for C30-50%GGBS.while, 43.9% of GWP, 40.5% of AP, 32.7% of EP, 32.2% of POCP and 49.4% of PEI non-re are achieved for C40-50%GGBS. Based on the preceding evaluation, it may be inferred that concrete mixtures including high-volume GGBS (50%) substantially reduce their environmental impact. Concurrently, these mixtures also save an equal amount of natural resources that maintain the ecological balance and environment soundness. Thus, it is feasible to create environmentally sustainable and clean concrete based on the appropriate application of replacing cement with GGBS.

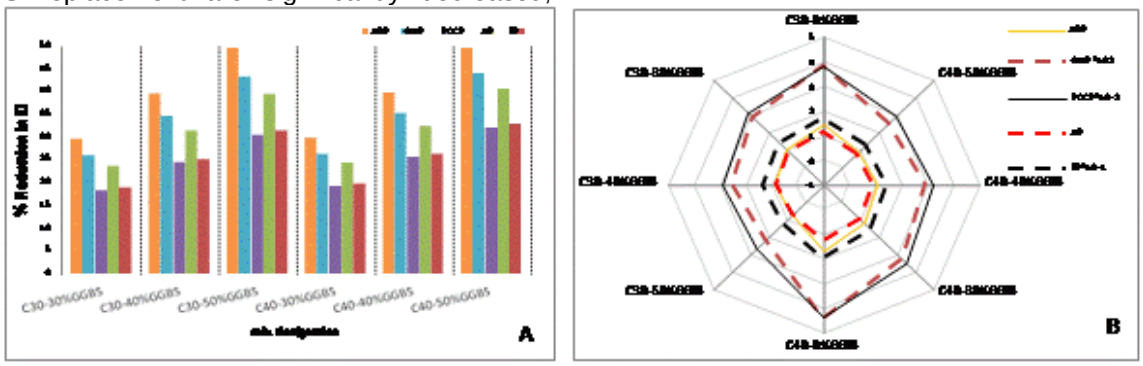

Figure 24. (A) Reduced environmental impact of concrete mixes than control mix (B) Environmental impact parameters of 1m³ reference and GGBS mixtures

4. CONCLUSIONS

Goal of this investigation was to see whether an optimal eco-friendly concrete with large volume GGBS would have better corrosion resistance than concrete of similar or greater strength, that reduces waste management issues and conserves natural resources for future generations. A comprehensive study of fresh, hardened and durability properties was carried out. This entailed creating eight concrete mixes of two grades, C30 and C40 concrete, which were then placed in a 5% chloride solution for impressed current testing. Principal findings can be inferred from the experimental results:

1. The incorporation of GGBS in concrete mixes resulted in increased slump values, indicating improved workability. This effect was evident in the setting time of cement paste, both initial and final setting times were extended with higher GGBS content.

2. The compressive strength of C30 and C40 concrete specimens improved with the replacement of GGBS content up to 40%, which can be considered as the optimum dosage of GGBS, and then decreased to 50% GGBS content. The other strength properties, such as the splitting tensile and flexural strength, also show similar variation as in the case of the compressive strength. Compared to reference mixes, the highest increase in compressive, splitting, and flexural strength was achieved by substituting 40% of OPC with GGBS.

3.The micro-structural analyses of the concrete paste samples confirm the variation in the strength properties of their respective concrete mixes. The microstructural analyses of C30-0%GGBS and 30-40%GGBS in terms of SEM revealed that replacing cement with GGBS improved the concrete microstructure and increased the ITZ's density.

4. The inclusion of GGBS has shown an excellent reduction in environmental impact (EI) in all aspects. Hence, the use of high-volume GGBS in concrete causes a significant reduction in EI in all respects. The C30-50%GGBS and C40-50 % GGBS mixture achieved the highest reduction in EI.

5. The electrical resistivity was found to increase with increasing GGBS replacement ratio in the concrete mixture, where the electrical resistivity was significantly improved. The C30-50%GGBS and C40-50%GGBS mixtures achieved electrical resistivity measurements of (41.63 and 74.03) kΩ.cm, respectively, at 90 days, which were higher than the values of the remaining six mixtures, significantly reducing the chances of corrosion. The reason behind this is the denser microstructure resulting from the formation of the secondary CSH gel.

6. In the mix designs containing GGBS, the porosity and water absorption were decreased compared to the reference mixes. The mix containing the highest cement replacement ratio with GGBS (50%) achieved the highest reduction in porosity and water absorption at 28 and 90 days. The C40-50%GGBS mix gave the lowest value of porosity and water absorption at 90 days compared to the rest of the mixes, which amounted to (2.47)% and (1.05)%, respectively.

7. The penetration depths of chloride ions decreased with increasing the percentage of slag replacement in the blast furnace. The experimental results indicated that the inclusion of GGBS in concrete mixtures led to a decrease in the penetration depth at 90 days between (8.79-3.74) mm, while the reference mixtures (C30-0%GGBS, C40-0%GGBS) recorded a penetration depth at 90 days of (31.34, and 20.38) mm, respectively. The C40-50%GGBS mixture recorded the lowest penetration depth at 90 days of (3.74) mm. As for the chloride ion migration coefficients, it followed the same pattern of penetration depth. The C30-50%GGBS and C40-50%GGBS mixtures recorded the highest decrease in the chloride ion migration coefficient at 90 days by (85.86, and 85.39)% compared to the reference mixtures (C30-0%GGBS and C40-0%GGBS).

8. The mass loss and corrosion rate of the reinforced steel embedded in the concrete diminished with increasing GGBS content, suggesting enhanced durability and longevity of the concrete. The results indicated that the concrete mixes with 50% GGBS had the greatest corrosion resistance over time, which was anticipated because the low permeability of the high GGBS addition, Lastly, after extracting and shot blasting rebars, the rebar of mix C30-50%GGBS was found to have corroded less than the rebar of mix C40-40%GGBS.

9. Based on the results of all the tests we have conducted, we conclude that it is possible to the optimum strength of the concrete C30 with 50%GGBS replacement can be rather depend instead of using a larger strength concrete with the same content of GGBS or leas, tends to result in carbon emission and cost savings whilst providing enhanced corrosion protection.

5. REFERENCES

[1] M. Valipour, M. Yekkalar, M. Shekarchi, S. Panahi (2014) Environmental assessment of green concrete containing natural zeolite on the global warming index in marine environments, J. Clean. Prod., vol. 65, pp. 418–423. https://doi.org/10.1016/j.jclepro.2013.07.055

[2] C. R. Gagg (2014) Cement and concrete as an engineering material: An historic appraisal and case study analysis, Eng. Fail. Anal., vol. 40, pp. 114–140.https://doi.org/10.1016/j.engfailanal.2014.02.004

[3] F. Pacheco-Torgal, R. E. Melchers, X. Shi, N. De Belie, K. Van Tittelboom, A. S. Perez (2017) Eco-efficient repair and rehabilitation of concrete infrastructures. Woodhead Publishing.

[4] R. Corral Higuera, S. P. Arredondo Rea, J. L. Almaral Sánchez, J. M. V. Gómez Soberón (2013) Chloride corrosion of embedded reinforced steel on concrete elaborated from recycled coarse aggregates and supplementary cement materials, Rev. Ing. construcción, vol. 28, no. 1, pp. 21–35. doI:10.4067/SO718-50732013000100002

[5] A. A. Hashim, N. S. Azeez, A. S. Naje, H. A. M. Al-Zubaidi (2021) Eco Friendly Enhancement of Self-Compacting Concrete Mechanical Properties using Metakaolin and Nanosilica, J. Green Eng., vol. 11, pp. 1748–1766. doi: 10.13140/RG.2.2.32434.72641

[6] A. Malakooti (2017) Investigation of concrete electrical resistivity as a performance based test. Utah State University http://dx.doi.org/10.13140/RG.2.2.28525.69603

[7] M. Velumani, R. Mohanraj, R. Krishnasamy, K. Yuvaraj (2023) Durability evaluation of cactus-infused M25 grade concrete as a bio-admixture, Period. Polytech. Civ. Eng., 67(4), 1066–1079. https://doi.org/10.3311/PPci.22050

[8] R. Mohanraj, S. Senthilkumar, P. Goel, R. Bharti (2023) A state-of-the-art review of Euphorbia Tortilis cactus as a bio-additive for sustainable construction materials, Mater. Today Proc.. https://doi.org/10.1016/j.matpr.2023.03.762

[9] U. M. Angst (2018) Challenges and opportunities in corrosion of steel in concrete, Mater. Struct., 51(1), 4-11. https://doi.org/10.1617/s11527-017-1131-6

[10] P. Padmapoorani, S. Senthilkumar, R. Mohanraj (2023) Machine learning techniques for structural health monitoring of concrete structures: A systematic review, Iran. J. Sci. Technol. Trans. Civ. Eng., 47(4), 1919–1931. https://doi.org/10.1007/s40996-023-01054-5

[11] M. G. Sohail, et al. (2020) Electrochemical behavior of mild and corrosion resistant concrete reinforcing steels, Constr. Build. Mater., 232, 117205. https://doi.org/10.1016/j.conbuildmat.2019.117205

[12] S. K. Verma, S. S. Bhadauria, S. Akhtar (2014) Monitoring corrosion of steel bars in reinforced concrete structures, Sci. world J., 2014(1), 957904. https://doi.org/10.1155/2014/957904

[13] A. A. Hashim, Z. kazem Rodhan, S. J. Abbas (2020) Fresh and hardened properties of self-compacting high performance concrete containing nano-metakaolin as a partial replacement, in IOP Conference Series: Materials Science and Engineering, IOP Publishing, p. 22036, doi 10.1088/1757-899X/928/2/022036

[14] F. Chen, H. Baji, C.-Q. Li (2018) A comparative study on factors affecting time to cover cracking as a service life indicator, Constr. Build. Mater., 163, 681–694. https://doi.org/10.1016/j.conbuildmat.2017.12.120

[15] A. A. Ramezanianpour, A. Pilvar, M. Mahdikhani, F. Moodi (2011) Practical evaluation of relationship between concrete resistivity, water penetration, rapid chloride penetration and compressive strength, Constr. Build. Mater., 25(5), 2472–2479. https://doi.org/10.1016/j.conbuildmat.2010.11.069

[16] K. TUUTTI (1982) Corrosion of steel in concrete, Swedish Cem. Concr. Res. Inst., vol. Report 4-8.

[17] R. R. Aveldaño, N. F. Ortega (2011) Characterization of concrete cracking due to corrosion of reinforcements in different environments, Constr. Build. Mater., 25(2), 630–637. doi.org/10.1016/j.conbuildmat.2010.07.029

[18] J.-K.Kim, J.-J.Yee, S.-H. Kee (2021) Electrochemical deposition treatment (Edt) as a comprehensive rehabilitation method for corrosion-induced deterioration in concrete with various severity levels, Sensors, vol. 21(18), 6287. https://doi.org/10.3390/s21186287

[19] K. M. Gopalakrishnan, R. Mohanraj, S. Southamirajan, S. Ramkumar (2024) Characterization of Euphorbia Tortilis Cactus Concrete Specimen by 3D X-ray Tomography, Russ. J. Nondestruct. Test., 60(6), 692–698. https://doi.org/10.1134/S1061830924601892

[20] M. F. M. Zain, H. B. Mahmud, A. Ilham, M. Faizal (2002) Prediction of splitting tensile strength of high-performance concrete, Cem. Concr. Res.,32(8), 1251–1258. doi.org/10.1016/S0008-8846(02)00768-8

[21] K. M. Rahla, R. Mateus, L. Bragança (2019) Comparative sustainability assessment of binary blended concretes using Supplementary Cementitious Materials (SCMs) and Ordinary Portland Cement (OPC), J. Clean. Prod., 220, 445–459. https://doi.org/10.1016/j.jclepro.2019.02.010

[22] D. M. Kannan, S. H. Aboubakr, A. S. El-Dieb, M. M. R. Taha (2017) High performance concrete incorporating ceramic waste powder as large partial replacement of Portland cement, Constr. Build. Mater., 144, 35–41. https://doi.org/10.1016/j.conbuildmat.2017.03.115

[23] T. Wu, S. T. Ng, J. Chen (2022) Deciphering the CO2 emissions and emission intensity of cement sector in China through decomposition analysis, J. Clean. Prod., 352, 131627. https://doi.org/10.1016/j.jclepro.2022.131627

[24] E. Stanaszek-Tomal (2009) Bacterial concrete as a sustainable building material?, Sustainability, 12(2), 696, https://doi.org/10.3390/su12020696.

[25] V. Penttala (2009) Causes and mechanisms of deterioration in reinforced concrete, in Failure, distress and repair of concrete structures, Elsevier, p. 3–31, https://doi.org/10.1533/9781845697037.1.3

[26] R. Siddique, M. I. Khan (2011) Supplementary cementing materials. Springer Science & Business Media. https://doi 10.1007/978-3-642-17866-5

[27] W. Matthes, et al. (2018) Ground granulated blast-furnace slag, Prop. Fresh Hardened Concr. Contain. Suppl. Cem. Mater. State-of-the-Art Rep. RILEM Tech. Comm. 238-SCM, Work. Gr. 4, 1–53. https://doi.org/10.1007/978-3-319-70606-1_1

[28] A. Aghaeipour, M. Madhkhan (2017) Effect of ground granulated blast furnace slag (GGBFS) on RCCP durability, Constr. Build. Mater., 141, 533–541. doi.org/10.1016/j.conbuildmat.2017.03.019

[29] M. D. A. Thomas, R. D. Hooton, A. Scott, H. Zibara (2012) The effect of supplementary cementitious materials on chloride binding in hardened cement paste, Cem. Concr. Res., 42(1), 1–7. https://doi.org/10.1016/j.cemconres.2011.01.001

[30] P. Purnell, L. Black (2012) Embodied carbon dioxide in concrete: Variation with common mix design parameters, Cem. Concr. Res., 42(6), 874–877.https:/doi.org/10.1016/j.cemconres.2012.02.005

[31] O. E. Babalola, et al. (2020) Mechanical and durability properties of recycled aggregate concrete with ternary binder system and optimized mix proportion, J. Mater. Res. Technol., 9(3), 6521–6532. https://doi.org/10.1016/j.jmrt.2020.04.038

[32] V. B. R. Suda, P. S. Rao (2020) Experimental investigation on optimum usage of Micro silica and GGBS for the strength characteristics of concrete, Mater. today Proc., 27, 805–811. https://doi.org/10.1016/j.matpr.2019.12.354

[33] BS EN 197-part 1 (2011), European Committee for Standardization, “Cement-part 1: Composition, specifications and conformity criteria for common cements

[34] BS EN. 15167 part 1 (2006), European Committee for Standardization, “Ground granulated blast furnace slag for use in concrete, mortar and grout - Part 1: Definitions, specifications and conformity criteria,”.

[35] S. C. Pal, A. Mukherjee, S. R. Pathak (2003) Investigation of hydraulic activity of ground granulated blast furnace slag in concrete,” Cem. Concr. Res., 33(9), 1481–1486. https://doi.org/10.1016/S0008-8846(03)00062-0

[36] R. N. Swamy (1997) Design for durability and strength through the use of fly ash and slag in concrete, Spec.Publ.,171, 1–72. doi: 10.14359/6090

[37] A. A. Ramezanianpour (2014) Cement replacement materials, Springer geochemistry/mineralogy, 10, 973–978.https://doi.org/10.1007/978-3-642-36721-2

[38] S. Kumar, et al. (2008) Mechanical activation of granulated blast furnace slag and its effect on the properties and structure of portland slag cement, Cem. Concr. Compos., 30(8), 679–685. https://doi.org/10.1016/j.cemconcomp.2008.05.005

[39] E. Özbay, M. Erdemir, H. İ. Durmuş (2016) Utilization and efficiency of ground granulated blast furnace slag on concrete properties–A review, Constr. Build. Mater., 105, 423–434. https://doi.org/10.1016/j.conbuildmat.2015.12.153

[40] ASTM C989-06, American Society for Testing and Materials (2006) Standard Specification for Ground Granulated Blast-Furnace Slag for Use in Concrete and Mortars,.

[41] BS EN 12620:2002, and +A1:2008 (2008) European Committee for Standardization, Aggregates for concrete.

[42] ASTM C494-11, American Society for Testing and Materials (2011) Standard Specification for Chemical Admixtures for Concrete,.

[43] BS EN 12350- 2, European Committee for Standardization(2009) Testing fresh concrete. Slump test.

[44] BS EN 196-3:2005+ A1:2008 part 3, European Committee for Standardization (2008) Methods of testing cement, Determination of setting times and soundness.

[45] BS EN 12390-3 part 3, European Committee for Standardization (2019) Testing hardened concrete, Compressive strength of test specimens.

[46] BS EN 12390-6 part 6, European Committee for Standardization (2009) Testing hardened concrete, Tensile splitting strength of test specimens.

[47] BS EN 12390-5 part 5, European Committee for Standardization (2009) Testing hardened concrete - Part 5: Flexural strength of test specimens,".

[48] ASTM C642-13, American Society for Testing and Materials (2013) Standard test method for density, absorption, and voids in hardened concrete.

[49] O. E. Gjørv (2009) Durability design of concrete structures in severe environments. CRC Press. https://doi.org/10.4324/9781482265903

[50] NT Build 492 (1999) chloride migration coefficient from non-steady-state migration experiments.

[51] W. Feng, A. Tarakbay, S. A. Memon, W. Tang, H. Cui (2021) Methods of accelerating chloride-induced corrosion in steel-reinforced concrete: A comparative review, Constr. Build. Mater., 289, 123165. doi.org/10.1016/j.conbuildmat.2021.123165

[52] S. Ahmad (2009) Techniques for inducing accelerated corrosion of steel in concrete, Arab. J. Sci. Eng., 34(2), 95-103.

[53] R. Kurda, J. D. Silvestre, J. de Brito (2018) Toxicity and environmental and economic performance of fly ash and recycled concrete aggregates use in concrete: A review," Heliyon, 4(4). http://dx.doi.org/10.1016/j.heliyon.2018.e00611

[54] T. H. Kim, S. H. Tae, C. U. Chae, W. Y. Choi (2016) The environmental impact and cost analysis of concrete mixing blast furnace slag containing titanium gypsum and sludge in South Korea, Sustainability, 8(6), 502. https://doi.org/10.3390/su8060502

[55] I. C. Thakur, N. Kisku, J. P. Singh, S. Kumar (2016) Properties of concrete incorporated with GGBS, Int. J. Res. Eng. Technol, 5, 275–281. http://dx.doi.org/10.12989/acc.2017.5.5.437

[56] S. Vediyappan, P. K. Chinnaraj, B. B. Hanumantraya, S. K. Subramanian (2021) An experimental investigation on geopolymer concrete utilising micronized biomass silica and GGBS, KSCE J. Civ. Eng., 25, 2134–2142. https://doi.org/10.1007/s12205-021-1477-8

[57] Z. Giergiczny (2019) Fly ash and slag, Cem. Concr. Res., 124, 105826. https://doi.org/10.1016/j.cemconres.2019.105826

[58] J. Ahmad, S. U. R. Rehman, O. Zaid, A. Manan, S. Beddu, M. Ahmad (2020) To study the characteristics of concrete by using high range water reducing admixture, IJMPERD, 10, 14271–14278.

[59] R. K. Majhi, A. N. Nayak, B. B. Mukharjee (2018) Development of sustainable concrete using recycled coarse aggregate and ground granulated blast furnace slag, Constr. Build. Mater., 159, 417–430. https://doi.org/10.1016/j.conbuildmat.2017.10.118

[60] A. Alhozaimy, A. Al-Negheimish, O. A. Alawad, M. S. Jaafar, J. Noorzaei (2012) Binary and ternary effects of ground dune sand and blast furnace slag on the compressive strength of mortar, Cem. Concr. Compos., 34, 6, 734–738. https://doi.org/10.1016/j.cemconcomp.2012.03.002

[61] [61]Z. Xu, et al. (2022) Promoting utilization rate of ground granulated blast furnace slag (GGBS): Incorporation of nanosilica to improve the properties of blended cement containing high volume GGBS, J. Clean. Prod., 332, 130096. https://doi.org/10.1016/j.jclepro.2021.130096

[62] H. Zhao, W. Sun, X. Wu, B. Gao (2015) The properties of the self-compacting concrete with fly ash and ground granulated blast furnace slag mineral admixtures, J. Clean. Prod., 95, 66–74. https://doi.org/10.1016/j.jclepro.2015.02.050

[63] A. M. Neville (2011) Properties of Concrete, 4th , London Pearson Educ. Ltd., 443(846) 444-451.

[64] S. K. Rao, P. Sravana, T. C. Rao (2016) Abrasion resistance and mechanical properties of Roller Compacted Concrete with GGBS, Constr. Build. Mater., 114, 925–933. https://doi.org/10.1016/j.conbuildmat.2016.04.004

[65] M. Manjunatha, D. Seth, K. Balaji (2021) Role of engineered fibers on fresh and mechanical properties of concrete prepared with GGBS and PVC waste powder–An experimental study, Mater. Today Proc., 47, 3683–3693. https://doi.org/10.1016/j.matpr.2021.01.605

[66] S. V. B. Reddy, P. S. Rao (2020) Experimental studies on mechanical properties and impact characteristics of ternary concrete with steel fiber, Mater. Today Proc., 27, 788–797. https://doi.org/10.1016/j.matpr.2019.12.344

[67] J. Kangwa, J. Kamau, A. Ahmed, P. Hirst, F. Hyndman (2017) Influence of rice husk ash density on the workability and strength of structural concrete, Eur. J. Eng. Res. Sci., 2(3), 36–43. https://doi.org/10.24018/ejers.2017.2.3.292

[68] N. Bheel, K. A. Kalhoro, T. A. Memon, Z. U. Z. Lashari, M. A. Soomro, U. A. Memon (2020) Use of marble powder and tile powder as cementitious materials in concrete, Eng. Technol. Appl. Sci. Res., 10, 2, 5448–5451. http://dx.doi.org/10.48084/etasr.3378

[69] V. Afroughsabet, L. Biolzi, T. Ozbakkaloglu (2017) Influence of double hooked-end steel fibers and slag on mechanical and durability properties of high performance recycled aggregate concrete, Compos. Struct., 181, 273–284. https://doi.org/10.1016/j.compstruct.2017.08.086

[70] L. A. Qureshi, B. Ali, A. Ali (2020) Combined effects of supplementary cementitious materials (silica fume, GGBS, fly ash and rice husk ash) and steel fiber on the hardened properties of recycled aggregate concrete, Constr. Build. Mater., 263, 120636. doi.org/10.1016/j.conbuildmat.2020.120636

[71] ACI 222R-01 (2001) Protection of Metals in Concrete against Corrosion, Am. Concr. Inst. Committee, Detroit,.

[72] A. Elahi, P. A. M. Basheer, S. V Nanukuttan, Q. U. Z. Khan (2010) Mechanical and durability properties of high performance concretes containing supplementary cementitious materials, Constr. Build. Mater., 24, 3, 292–299. https://doi.org/10.1016/j.conbuildmat.2009.08.045

[73] O. Sengul, O. E. Gjørv (2008) Electrical resistivity measurements for quality control during concrete construction, ACI Mater. J., 105(6), 541. DOI: 10.14359/20195

[74] C. Bhojaraju, S. S. Mousavi, V. Brial, M. DiMare, C. M. Ouellet-Plamondon (2021) Fresh and hardened properties of GGBS-contained cementitious composites using graphene and graphene oxide, Constr. Build. Mater., 300, 123902. https://doi.org/10.1016/j.conbuildmat.2021.123902

[75] O. Kayali, M. S. H. Khan, M. S. Ahmed (2012) The role of hydrotalcite in chloride binding and corrosion protection in concretes with ground granulated blast furnace slag, Cem. Concr. Compos., vol. 34, no. 8, pp. 936–945. https://doi.org/10.1016/j.cemconcomp.2012.04.009

[76] S. G. Ytterdal (2014) The effect of fly ash and ggbfs as cement replacement on chloride binding and ingress in mortar samples. Institutt for bygg, anlegg og transport.

[77] A. S. Natanzi, B. J. Thompson, P. R. Brooks, T. P. Crowe, C. McNally (2021) Influence of concrete properties on the initial biological colonisation of marine artificial structures, Ecol. Eng., 159, 106104. https://doi.org/10.1016/j.ecoleng.2020.106104

[78] J. Wang, E. Liu (2020) The relationship between steady-state chloride diffusion and migration coefficients in cementitious materials, Mag. Concr. Res., 72(18), 1016–1026. https://doi.org/10.1680/jmacr.18.00286

[79] J. Ahmad, et al. (2022) A comprehensive review on the ground granulated blast furnace slag (GGBS) in concrete production, Sustainability, 14(14), 8783. https://doi.org/10.3390/su14148783

[80] K. Kopecskó, G. L. Balázs (2017) Concrete with improved chloride binding and chloride resistivity by blended cements, Adv. Mater. Sci. Eng., 1, 7940247. https://doi.org/10.1155/2017/7940247

[81] J. Zhao, E. D. Shumuye, Z. Wang (2021) Effect of slag cement on concrete resistance against combined exposure to freeze-thaw and chloride ingress, J. Eng. Sci. Technol., 16(6), 4687–4706. http://dx.doi.org/10.2478/ncr-2024-0012

[82] ASTM G1, American Society for Testing and Materials (2003) Standard Practice for Preparing, Cleaning, and Evaluation Corrosion Test Specimens,".

[83] W. Shen, et al. (2017) Cement industry of China: Driving force, environment impact and sustainable development, Renew. Sustain. Energy Rev., 75, 618–628. https://doi.org/10.1016/j.rser.2016.11.033

[84] M. U. Hossain, C. S. Poon, I. M. C. Lo, J. C. P. Cheng (2016) Comparative environmental evaluation of aggregate production from recycled waste materials and virgin sources by LCA, Resour. Conserv. Recycl., 109, 67–77. https://doi.org/10.1016/j.resconrec.2016.02.009

[85] R. K. Majhi, A. N. Nayak (2020) Production of sustainable concrete utilising high-volume blast furnace slag and recycled aggregate with lime activator, J. Clean. Prod., 255, 120188. https://doi.org/10.1016/j.jclepro.2013.07.055

IZVOD

VISOKOKVALITETNI EKOLOŠKI BETON SA POBOLJŠANOM ČVRSTOĆOM, PENETRACIJOM HLORIDNIH JONA I OTPORNOŠĆU NA KOROZIJU ZAHVALJUJUĆI VELIKOJ KOLIČINI MLEVENE GRANULIRANE ZGURE VISOKE PEĆI (GGBS)

Ovo istraživanje ima za cilj proizvodnju betona koji zadovoljava parametre čvrstoce na pritisak, ima najmanji uticaj na životnu sredinu i otporan je na prodiranje hloridnih jona i koroziju. U ovom istraživanju korišcene su različite zapremine zamene cementa šljakom (GGBS) (30, 40 i 50)% mase cementa za dve klase betona, C30 i C40. Svježi testovi (slijeganje, početno i konačno vrijeme vezivanja), očvršcavanje (čvrstoca na pritisak, cijepanje i savijanje) i izdržljivost (poroznost, upijanje vode, gustina, dubina prodiranja, koeficijent migracije hloridnih jona, električna otpornost, brzina korozije, gubitak mase, širina prsline usled korozije i analiza mikrostrukture).

Takođe je procenjen uticaj komponenti betona na životnu sredinu u svakoj mešavini. Tehnika impresionirane struje povecala je koroziju armature u uzorcima betona potopljenim u 5% natrijum hlorida. Zamena cementa GGBS-om za 30–50% povecala je vreme vezivanja i poboljšala sve kvalitete očvršcavanja. Mehanički kvaliteti su senajviše poboljšali pri 40% GGBS, sa C30 mešavinama na pritisak, zatezanje i savijanje za 29,3%, 38,7% i 15,8% na 90 dana. Uporedite 21,3%, 19,2% i 16,2% na 90 dana za kombinacije C40 sa referentnom smešom. Snaga je neznatno smanjena na 50% GGBS, ali je ostala veca od referentne mešavine. Međutim, stopa zamene od 50% GGBS najbolje je poboljšala izdržljivost, mikrostrukturu i ekološku efikasnost. Smeša C30-50% GGBS je idealna jer je ispunjavala zahteve dizajna C30 i C40, imala je najbolje poboljšanje u poroznosti i apsorpciji vode, najmanju penetraciju hlorida i najbolje performanse protiv korozivnih sredina od šest smeša osim C40-50 % GGBS. Pored toga, to je najmanje štetna kombinacija po životnu sredinu.

Ključne reči: *GGBS,prodor hloridnih jona, otpornost na koroziju, mikrostruktura betona, uticaj na životnu sredinu, trajnost*

Naučni rad
Rad primljen: 21.12.2024.
Rad prihvaćen: 15.01.2025.

Akram O. Kadhum *https://orcid.org/0009-0009-6306-6940*
Abbas S. AL-Ameeri *https://orcid.org/0000-0002-5852-0450*
Shaker J. Edrees *https://orcid.org/0000-0002-9996-1279*
Muhammad I. Rafiq *https://orcid.org/0000-0003-1175-9576*